the time at which the Stokes photon strikes D_s. Tracking the evolution of the Stokes operator through the optical setup $s(t'_s) = s_L(t_s) + e^{i\varphi_s} s_R(t_s)$ [neglecting normalization and global phases; see (*18*)], we obtain the state

$$E|\psi_s\rangle = \left[b_L^\dagger(t_s) + e^{-i\varphi_s} b_R^\dagger(t_s)\right]|\mathrm{vac}_{\mathrm{vib}}\rangle \quad (2)$$

which is an entangled state of the two diamonds at t_s containing a single phonon excitation distributed across the two crystals.

Observing a Stokes-scattered photon at D_s therefore allows us to infer the presence of entanglement between the diamonds. We then test this inference by directing strong probe pulses into the crystals at a time $T = 350$ fs after t_s, which is short compared to the coherence lifetime of 7 ps (*19*). Unlike similar experiments with atomic ensembles, the diamonds must be probed before the Stokes photon has reached D_s (*18*). The conventional time ordering could be recovered with the use of a chip-scale interferometer (*20*) and fast detectors (*21*). With small probability $|\varepsilon_a|^2 << 1$ the phonon is converted into a 40-THz blue-shifted anti-Stokes photon, $b \rightarrow b + \varepsilon_a a$, so that the joint state of the diamonds and anti-Stokes modes is

$$|\psi_a\rangle = \{b_L^\dagger(t_a) + e^{-i\varphi_s} b_R^\dagger(t_a) + \varepsilon_a\left[a_L^\dagger(t_a) + e^{-i\varphi_s} a_R^\dagger(t_a)\right]\}|\mathrm{vac}\rangle \quad (3)$$

where a is the annihilation operator for an anti-Stokes photon, and $t_a = t_s + T$. The anti-Stokes modes are combined on a polarizing beamsplitter, and interfered, with a controllable phase φ_a, by means of a half-wave plate and another polarizing beamsplitter. The numbers of anti-Stokes photons, $N_\pm$, that are detected emerging from the two output ports are given by $|\langle \mathrm{vac}|a_\pm(t'_a)|\Psi_a\rangle|^2 \propto \varepsilon_a^2 \sin^2[(\varphi_a + \varphi_s + \pi \pm \pi)/2]$, where $a_\pm(t'_a) = [a_L(t_a) \pm e^{i\varphi_a} a_R(t_a)]/\sqrt{2}$ and t_a' is the time at which anti-Stokes photons are detected. We use the copropagating pump and probe fields to actively stabilize φ_s and φ_a separately, so that the entanglement generation and verification

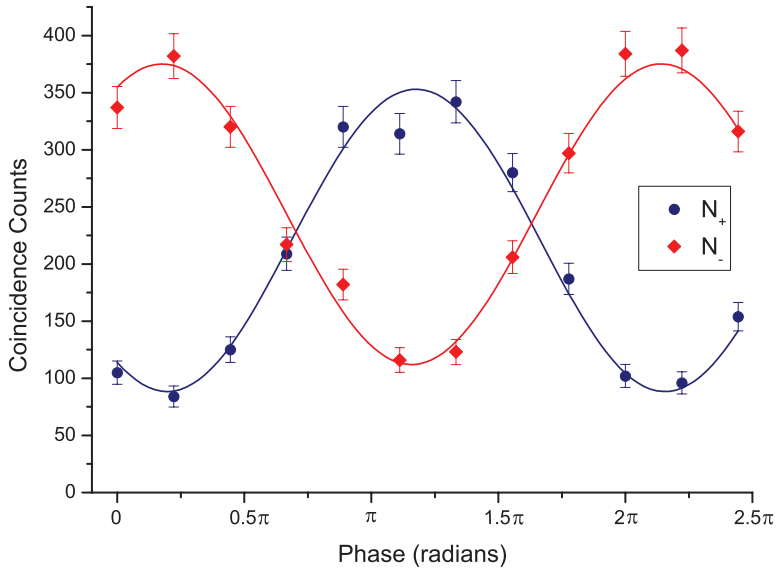

Fig. 2. Coincidence between herald and readout photons. The visibility is $V = (61 \pm 3)\%$ for N_+ and $V = (55 \pm 3)\%$ for N_-. The difference in visibility between the measurement sets we attribute to the different rate of accidental coincidences between the two detectors. Error bars on the plot are estimated from the standard deviation of a Poissonian process.

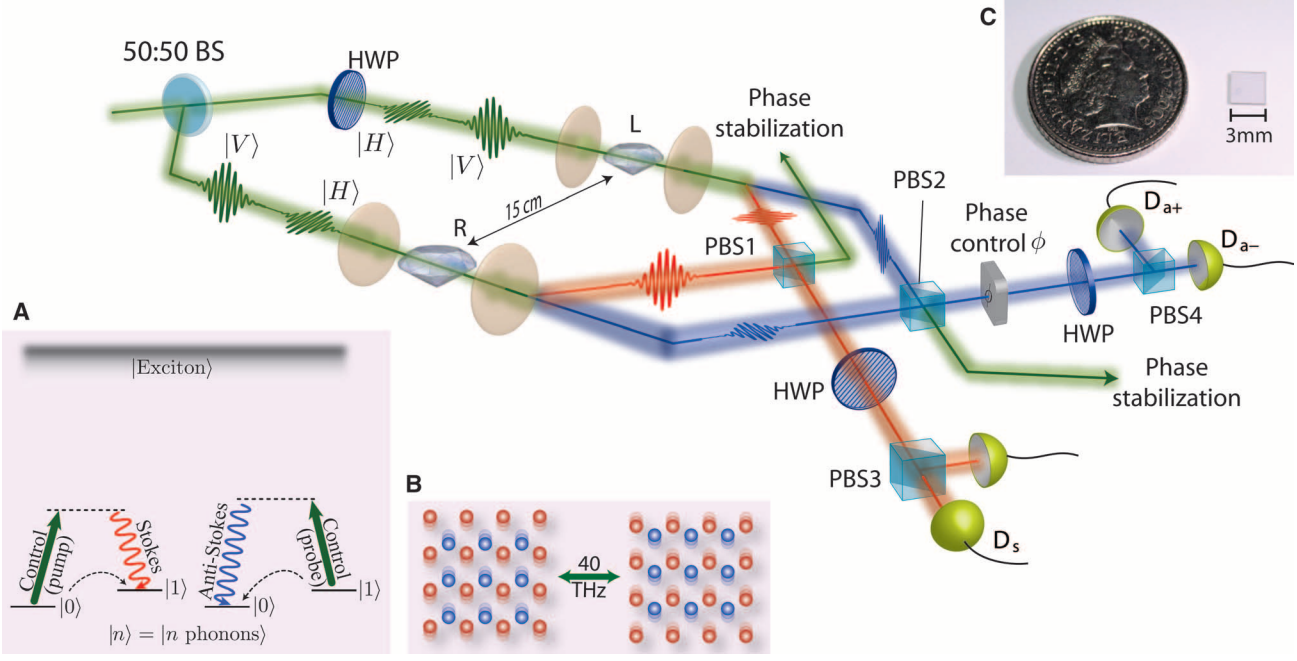

Fig. 1. Schematic of the experimental layout for generating entanglement between two diamonds. A pump pulse is split by the beamsplitter BS and focused onto two spatially separated diamonds. Optical phonons are created by spontaneous Raman scattering, generating the orthogonally polarized heralding Stokes fields s_L, s_R [see inset (**A**): $|n\rangle$ represents phonon number states in diamond]. Polarization beamsplitter PBS1 combines the spatial paths, and the half-wave plate HWP rotates and mixes the fields on PBS3, which are then directed into the single-photon detector D_s. A probe pulse, with programmable delay, coherently maps the optical phonon into the orthogonally polarized anti-Stokes fields a_L, a_R [see inset (A)], which are similarly combined and mixed on PBS2 and PBS4, and detected on the detectors D_{a+}, D_{a-}. The relative phase φ_a between the fields $a_{L,R}$ is controlled by a sequence of quarter- and half-wave plates (*18*). Rejected pump beams from PBS1,2 are used to stabilize the interferometer. Displacements of neighboring atoms from their equilibrium positions are anticorrelated in the optical phonon mode [see inset (**B**)], with a vibrational period of 25 fs in diamond. Inset (**C**) shows one of the diamond samples, with a coin for scale.